THE JOURNAL OF PHYSICAL CHEMISTRY Letters

Letter

pubs.acs.org/JPCL

Isotope-Dependent Rotational States Distributions Enhanced by Dynamic Resonance States: A Comparison Study of the F + HD → HF(v_{HF} = 2) + D and F + H_2 → HF(v_{HF} = 2) + H Reaction

Tao Wang,[†] Tiangang Yang,[†] Chunlei Xiao,*[,†] Zhigang Sun,*[,†,‡] Long Huang,[†] Dongxu Dai,[†,‡] Xueming Yang,*[,†,‡] and Dong H. Zhang*[,†,‡]

[†]State Key Laboratory of Molecular Reaction Dynamics and Center for Theoretical and Computational Chemistry, Dalian Institute of Chemical Physics, Chinese Academy of Sciences, Dalian 116023, People's Republic of China

[‡]Center for Advanced Chemical Physics, University of Science and Technology of China, 96 Jinzhai Road, Hefei 230026, People's Republic of China

Supporting Information

ABSTRACT: An interesting trimodal structure in the HF (v' = 2) rotational distribution produced by the F + HD (v = 0, j = 0) reaction, but monomodal structure in the HF (v' = 2) rotational distribution produced by the F + H_2 (v = 0, j = 0) reaction, were observed using a high-resolution crossed molecular beam apparatus. The rotational states of product HF (v' = 2) are much hotter in the F + HD reaction. It is uncovered that the observations are due to the dominant role of the dynamical resonance states in these two isotopic reactions. The angular potential well in the region of the resonance state of the F + HD reaction is much deeper and supports wave function with high angular kinetic energy, which in turn comes from different H tunneling processes in the F + HD and F + H_2 reaction.

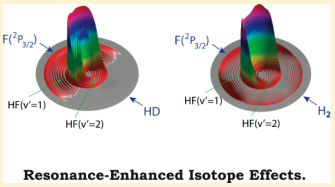

Resonance-Enhanced Isotope Effects.

SECTION: Kinetics and Dynamics

The reaction F + H_2 → HF + H and its isotopes are the main prototypes of an exothermic elementary chemical reaction, in which the existence of dynamics resonance attracted enormous experimental and theoretical studies over the past decades.[1−21] The nomenclature "resonance" refers to a transient metastable species produced in a reactive scattering, which results in peaks in the excitation functions, namely the reaction probabilities as a function of collision energy. Its observation and assignment in scattering experiments usually are difficult because the coherent summation of many partial waves tends to wash out most of the resonance structures. However, disclosure of the resonance states is essential to us for understanding the role of quasibound states in a chemical reaction with unique clarity.

In the early 2000s, Liu and co-workers carried out a detailed crossed molecular beam study on the F + HD reaction and observed a clear step in the total excitation function at about 0.5 kcal/mol for the F + HD (v = 0) → HF + D reaction.[15,18,19] In 2006, Qiu et al. observed forward scattering HF (v' = 2) product from the F + H_2 (v = 0) reaction at a collision energy of 0.52 kcal/mol, which was attributed to the interference between two reactive resonance states.[17] In 2008, Ren et al. carried out a full quantum state resolved reactive scattering study on the F($^2P_{3/2}$) + HD (v = 0, j = 0) → HF + D reaction, in an effort to probe the resonance potential experimentally, using the high resolution and highly sensitive H atom Rydberg tagging method.[21] A new ab initio potential energy surface (PES) (named as Fu−Xu−Zhang (FXZ) PES[22]) then was constructed by using the spin-unrestricted coupled cluster method with all single and double excitations and perturbative accounts of triple excitations [UCCSD(T)][21,22] in order to accurately describe the observed reactive resonances. Quantum dynamics studies show that the FXZ PES is able to describe very well the resonance states in both the F + H_2 and F + HD reaction,[21] and the slow-down mechanism in the F + H_2 → HF (v' = 3) + H reaction.[20] In the last year, a reactive scattering resonance state in the F + HD (v = 1) reaction was observed, which in turn was investigated using quantum reactive scattering theory on a more accurate Chen−Sun−Zhang (CSZ) PES[23] and was found to be only accessible to a vibrationally excited reactant.[24]

In the work by Ren et al.,[21] there is an interesting trimodal structure in the experimentally measured rotational state distribution of product HF (v' = 2) from the F + HD (v = 0, j = 0) reaction at a collision energy of 0.48 kcal/mol. The theoretical prediction based upon the FXZ PES in that work agrees with the experimental results well. However, how such structure arises in this reaction remains unclear to us. Similar rotational states distributions of the product HF (v' = 2) from the F + HD (v = 0, j = 0) reaction in the collision energy range 0.40−1.18 kcal/mol were measured by Lee et al. [18] also.

In the interest of understanding the physical mechanism of such trimodal structure, we carried out a high resolution crossed molecular beam D atom Rydberg tagging experiment at

Received: July 14, 2014
Accepted: August 20, 2014
Published: August 20, 2014

 © 2014 American Chemical Society dx.doi.org/10.1021/jz501460k | J. Phys. Chem. Lett. 2014, 5, 3049−3055

a collision energy of 0.44 kcal/mol and full quantum reactive scattering numerical calculations on the more accurate CSZ PES for studying the role of the reactive resonance in the F + HD ($v = 0, j = 0$) reaction, which has been assigned in previous studies.[15,21] In order to obtain a deeper physics picture of the role of the resonance states in the F + HD reaction, a high resolution crossed molecular beam H atom Rydberg tagging experiment and theoretical analysis were also carried out on the F + H_2 reaction at a collision energy of 0.19 kcal/mol for comparison. The reasons for choosing these two collision energies in the present work will be given below.

The experiment was conducted on a crossed beam machine with a rotatable fluorine (F) atom beam source and a fixed HD/H_2 molecular beam source.[25,26] By changing the crossing angle between the two beams, the collision energy could be tuned continuously.

The F atom was generated by a double-stage pulsed discharge from 5% F_2 premixed in Ne.[27] Both the ground $F(^2P_{3/2})$ and spin−orbit excited $F^*(^2P_{1/2})$ atoms were produced in the mixture, and the ground state F atom is found to be predominantly (F:F* ∼10.7). In the time-of-flight (TOF) spectra, there is a small signal coming from the reaction of the excited state $F^*(^2P_{1/2})$ atom with the diatomic reagent H_2/HD ($v = 0, j = 0$), which is discernible from that of the reaction with the ground state F atom in the F + H_2 reaction at the collision energy of 0.19 kcal/mol but is negligible in the F + HD reaction at the collision energy of 0.44 kcal/mol (Figure S1 in the Supporting Information).

The HD/H_2 beam was produced by pulsed supersonic expansion of pure HD/H_2 gas at liquid nitrogen temperature. After supersonic expansion, most of HD/H_2 molecules in the beam were in the lowest ($v = 0, j = 0$) state.

The CSZ PES was constructed using the hierarchical construction scheme.[21,22] To include the higher order excitation level of coupled cluster energy, we include the UCCSDT(2)Q-UCCSD(T) correction term V_4 to the FXZ PES based on 775 high level ab initio calculations, using the basis set AVQZ for the F atom and VQZ for the H atoms. This part of ab initio calculation was accomplished with the NWChem[28] package. Extensive study does indicate that the current PES is more accurate than previous version.[24,29] The current PES does not need any scaling factor to the original ab initio energy points.

Both the time-dependent wavepacket method using reactant Jacobi coordinates[30] and the time-independent method using hyperspherical coordinates[31] were applied to calculate the state-to-state information on the CSZ PES.

The 3D polar plot of the experimental differential cross sections (DCS) at a collision energy of E_c = 0.44 kcal/mol, which was constructed from the time-of-flight (TOF) spectra of the D atom from the reaction of F + HD ($v = 0, j = 0$) → HF ($v' = 1$ and 2, j') + D measured using the D atom Rydberg tagging technique, is shown in Figure 1B. In order to produce this 3D plot, the TOF spectra of the D atom was measured at many laboratory angles with an interval of 10°. The 3D DCS indicates that the product HF was scattered in the backward direction. Similar experimentally measured 3D DCS but for the reaction of the F + H_2 reaction at a collision energy of 0.19 kcal/mol is also plotted in Figure 1D.

Theoretical 3D polar DCS of the reaction of F + HD ($v = 0, j = 0$) → HF($v' = 1$ and 2, j') + D at a collision energy of 0.44 kcal/mol are shown in Figure 1A, along with that of the reaction of F + H_2 ($v = 0, j = 0$) → HF($v' = 1$ and 2, j') + H at a collision energy of 0.19 kcal/mol in Figure 1C. Comparing with the corresponding experimental DCS in Figure 1, we see that the DCS predicted by the CSZ PES can satisfactorily reproduce the experimental observations and only exhibit small differences in the backward scattering direction for the DCS of the F + HD reaction and in the sideways scattering direction for the DCS of the F + H_2 reaction. The experimentally measured, and theoretically predicted, rotational states distributions of product HF ($v' = 2$) of the two reactions are shown in Figure 2A and B, which agree with each other satisfactorily also. Therefore, it is safe to explain the physical mechanism of the experimental observation and to predict the reaction based upon the quantum reactive scattering results using the CSZ PES.

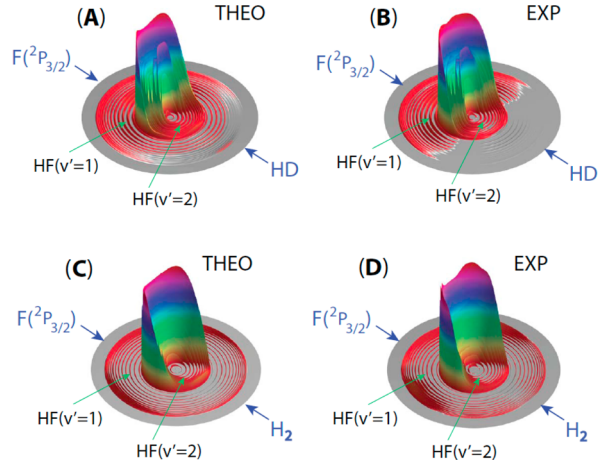

Figure 1. Experimental and theoretical 3D polar plots for the product ro-vibrational state resolved translational energy and angular distributions for the F + HD → D + HF reaction at a collision energy of 0.44 kcal/mol (A and B) and for the F + H_2 → H + HF reaction at a collision energy of 0.19 kcal/mol (C and D).

The total reaction probability with different values of the total angular momentum J_{total} of these two reactions, as a function of collision energy, are given in Figure 2C and D, and the total ICS of product HF ($v' = 2$) was plotted in Figure S2 of the Supporting Information. It is observed that, up to collision energy of 1.0 kcal/mol for the reaction of F + HD, the reaction mainly occurs through a reactive resonance state. However, for the reaction of F + H_2, the reaction with collision energy up to 0.37 kcal/mol occurs through a reactive resonance state. Therefore, the F + HD reaction with collision energy below 1.0 kcal/mol and the F + H_2 reaction with collision energy below 0.37 kcal/mol are completely mediated by these two reactive resonance states, which actually are the lowest resonance states for these two reactions, respectively.[16,17] The collision energy of 0.19/0.44 kcal/mol centers at about the middle of the collision energy range where the resonance state dominates for the F + H_2/HD reaction, which explains why we choose the collision energy of 0.19/0.44 kcal/mol in this work for illustration.

For the reaction of F + HD, at a collision energy of 0.44 kcal/mol, most of the product was produced by the first four partial waves. The width of the resonance peak is about 0.081 kcal/mol, which suggests that the lifetime of the resonance state is about 187 fs. Also, the rotational constant B_0 for the resonance state was found to be 0.0054 kcal/mol, corresponding to a rotational period of 8830 fs. Therefore, the resonance complex does not rotate fast enough with J_{total} = 2 or 3, which have the largest contribution to the ICS, to bring the product into

dx.doi.org/10.1021/jz501460k | J. Phys. Chem. Lett. 2014, 5, 3049−3055

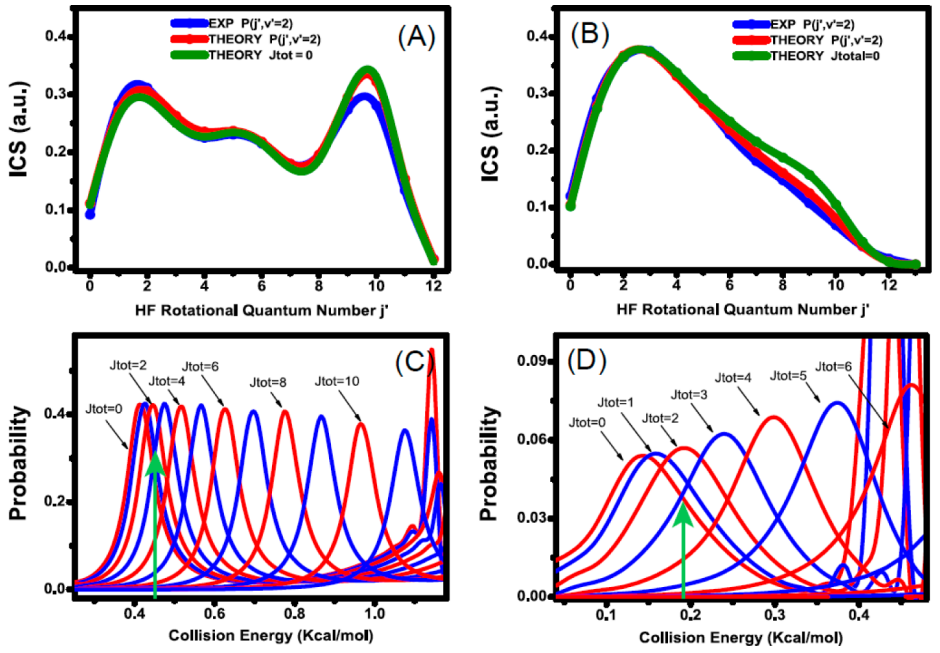

Figure 2. (A) and (B) Experimental and theoretical rotational state distribution of product HF ($v' = 2$) of reaction F + HD at a collision energy of 0.44 kcal/mol and F + H_2 at a collision energy of 0.19 kcal/mol and rotational state-resolved reaction probability with total angular momentum $J_{total} = 0$. Please be noted that the vertical axis labels are not meaningful for the result with $J_{total} = 0$. (C) and (D) Theoretical total reaction probability of the F + HD ($v = 0$, $j = 0$) → HF + D and F + H_2 ($v = 0$, $j = 0$) → HF + H reaction, as a function of collision energy with different values of total angular momentum J_{total}. The green lines with arrow in (C) and (D) indicate the collision energy positions where the experiments were conducted.

forward direction. As a result, we observe the product dominantly in the backward direction, as shown in Figure 1.

A similar analysis is applicable to the experimentally observed DCS of the F + H_2 reaction. At a collision energy of 0.19 kcal/mol, most of product was also produced by the first four partial waves. The width of the resonance peak is about 0.124 kcal/mol; thus, the resonance state has a shorter lifetime of about 123 fs. The rotational constant B_0 for the resonance state is larger (0.0081 kcal/mol), yielding a shorter rotational period of 5900 fs. Therefore, the resonance complex in the F + H_2 is not able to bring the product into forward direction either.

The final product rotational state distribution of HF ($v' = 2$) at a collision energy of 0.44 kcal/mol for the F + HD reaction and 0.19 kcal/mol for the F + H_2 reaction, calculated from single partial wave with total angular momentum $J_{total} = 0$, is given in Figure 2 also. We see that the relative rotational state distribution of HF ($v' = 2$) with $J_{total} = 0$ essentially agrees with the rotational state-resolved integral cross section (ICS) for both reactions. We further find that for these two reactions, the relative rotational state distribution of HF ($v' = 2$) with $J_{total} > 0$ is similar to that with $J_{total} = 0$, which implies that the rotational state distribution of HF ($v' = 2$) nearly does not vary with collision energy up to 0.37 kcal/mol for the F + H_2 reaction and 1.0 kcal/mol for the F + HD reaction, as shown in Figure S3 of the Supporting Information. Therefore, the significant difference in the rotational states distribution of product HF ($v' = 2$) between these two reactions, at a collision energy of 0.19 kcal/mol for the F + H_2 reaction and 0.44 kcal/mol for the F + HD reaction must be due to the reactive resonance (0.44−0.19 = 0.25 kcal/mol is only about two times of the energy difference between HF ($j' = 0$) and HF ($j' = 1$), which is about 0.114 kcal/mol).

In order to understand how the resonance states control the rotational state distribution of product HF ($v' = 2$) in these two reactions at the studied collision energies, we can effectively analyze the corresponding reactive resonance wave function with only $J_{total} = 0$.

The dynamical resonance wave functions in a reactive process was calculated by a rigorous and convenient method, a simple time-to-energy Fourier transform of the time-dependent wave function at the resonance peak. This method is different from the spectral quantization method[32] where a carefully designed initial wave function was used to obtain the time-independent wave function at the energies, which exhibit resonance peaks, by a Fourier transform of the time-propagated initial wave packet, as applied in a previous study on the resonance in F + HD reaction.[15]

The 2D calculated resonance wave function of the F + HD reaction as a function of R_{D-HF} and r_{HF} of product Jacobi coordinates at the resonance peak with collision energy of 0.383 kcal/mol for $J_{total} = 0$ is given in Figure 3A. The angular degree of freedom has been integrated out. It is seen there that the resonance wave function well localizes around (R_{D-HF}, r_{HF})

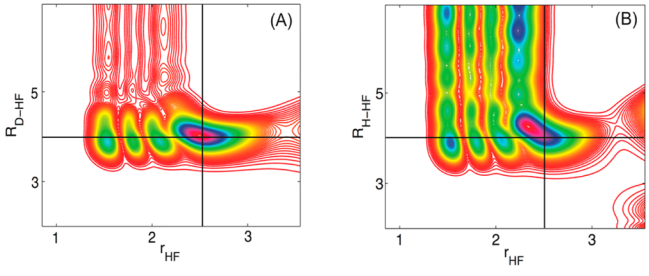

Figure 3. 2D wave functions of the dynamical resonance state at a collision energy of 0.383 kcal/mol for the F + HD reaction (A) and at of collision energy of 0.115 kcal/mol for the F + H_2 reaction (B) with $J_{total} = 0$ as a function of $R_{D/H-HF}$ and r_{HF}.

dx.doi.org/10.1021/jz501460k | J. Phys. Chem. Lett. 2014, 5, 3049−3055

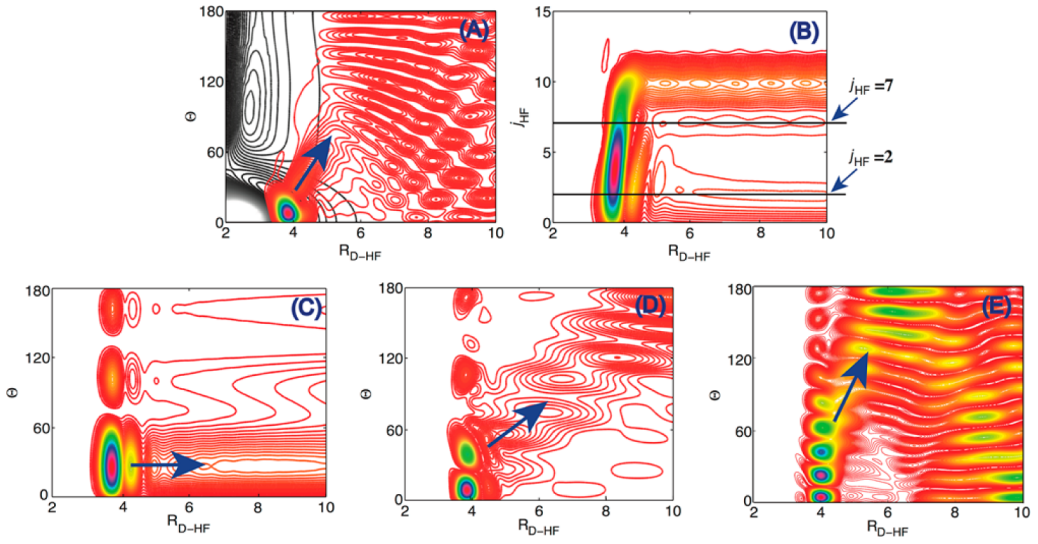

Figure 4. (A) 2D wave functions of the dynamical resonance state at a collision energy of 0.383 kcal/mol with $J_{total} = 0$ as a function of R_{D-HF} and θ, after projected the resonance wave function into vibrational state of HF ($v' = 2$). 2D PES with r_{HF} fixed at 2.5 au is presented as black contour lines. (B) The same wave function as in (A) but as a function of R_{D-HF} and rotational quantum number j'_{HF}. (C), (D), and (E) are the components of the wave function in (A) of j'_{HF} = 0−2, 3−7, and 8−14, respectively. They produce "dissociation" fluxes with rather different starting positions and directions.

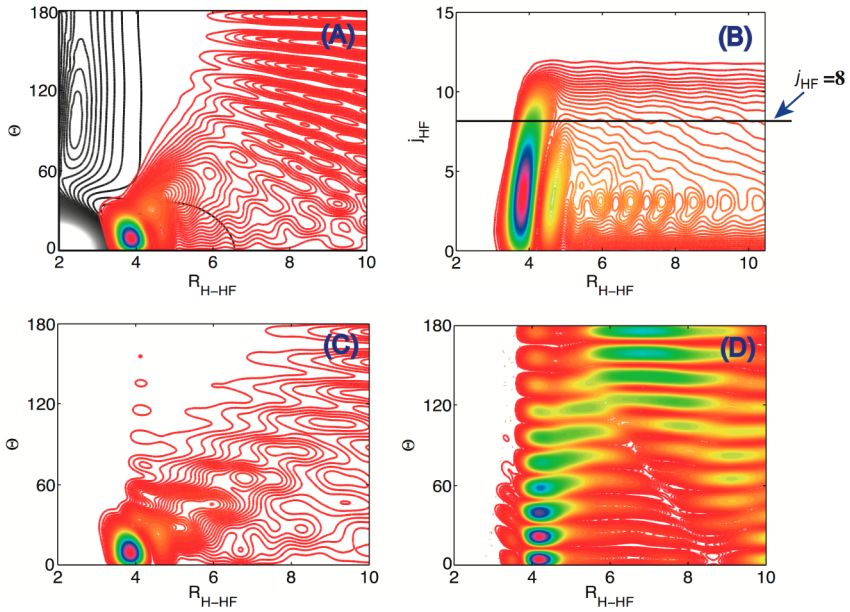

Figure 5. (A) 2D wave functions of the dynamic resonance state of the F + H_2 reaction at a collision energy of 0.115 kcal/mol with $J_{total} = 0$ as a function of R_{H-HF} and θ, after projected the resonance wave function into vibrational state of HF ($v' = 2$). 2D PES with r_{HF} fixed at 2.3 au is presented as black contour lines. (B) The same wave function as in (A) but as a function of R_{H-HF} and rotational quantum number j'_{HF}. (C) and (D) are the components of the wave function in (A) of j_{HF} = 0−8 and 9−14, respectively. In the resonance region, negligible part of the wave function acquires high angular kinetic energy (refer Figure 6), in contrast with panel (E) of Figure 4

= (4.0, 2.5) au and has clearly three nodes along r_{HF}. Therefore, it can be safely assigned as (003) state, since there is no node along angular degree of freedom.[16,21] Similar 2D resonance wave function of the F + H_2 reaction as a function of R_{H-HF} and r_{HF} at the resonance peak with collision energy of 0.115 kcal/mol for $J_{total} = 0$ is given in Figure 3B. Different from the resonance wave function in the F + HD reaction, the wave function in Figure 3B peaks around (R_{H-HF}, r_{HF}) = (4.2, 2.3) au and can also be assigned as (003) state,[17] but it is not so well localized. It is noted here that in the asymptotic region the wave function in Figure 3B has characteristics of $v_{HF} = 3$ due to the resonance wave function with a tail extending well into the region where H and HF are well separated, but the total available energy is not enough to open the channel of the product HF ($v_{HF} = 3$).

The 2D plots of the $v_{HF} = 2$ component of the resonance wave function of the F + HD reaction as a function of R_{D-HF} and θ are presented in Figure 4A, along with the 2D contour plot of the PES with r_{HF} fixed at 2.5 au where the resonance wave functions have largest amplitude. The $v_{HF} = 2$ component was calculated by projecting the calculated reactive resonance

dx.doi.org/10.1021/jz501460k | J. Phys. Chem. Lett. 2014, 5, 3049−3055

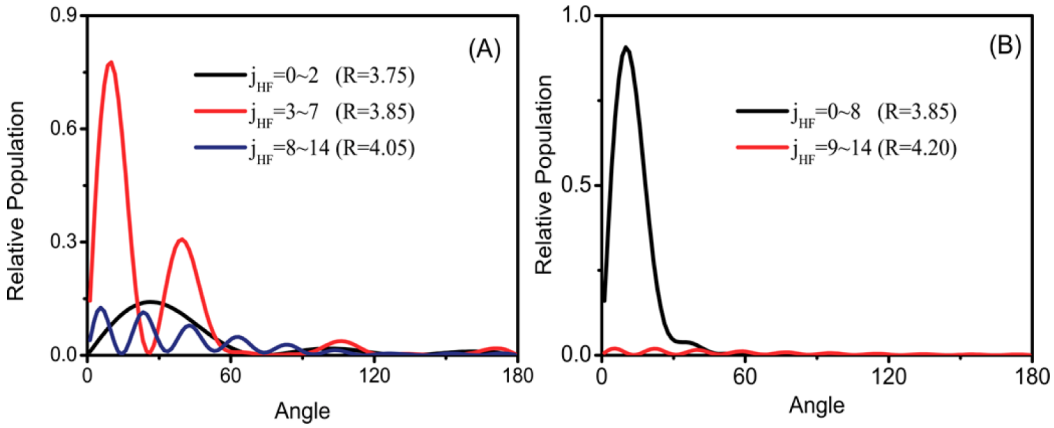

Figure 6. One-dimensional wave functions $|\varphi(\theta)|^2$ of the components obtained by the same decomposition as in Figures 4 and Figure 5, at fixed R where it exhibits largest amplitude for the F + HD (A) and F + H_2 (B) reaction.

wave function with the corresponding vibrational eigenfunction of the product HF.

From the figure, it is seen that the wave function "decaying" away from the region, where the wave function exhibits characteristics of a quasibound state, that is, the resonance region, has large angular momentum since it moves fast along the angular degree of freedom as it goes to asymptotic region, in the direction indicated by an arrow in Figure 4A. Theoretical results indicate that there is about 95% of the product depositing into HF (v_{HF} = 2), which suggests that the interaction between vibrational states in this resonance region is weak, in contrast with the strong coupling in the angular degree of freedom. The plot in Figure 4B also informs us that, as soon as the wave function leaves the resonance region, the rotational state distribution is determined. This fact suggests that the angular shape of the PES right after the resonance region is quite similar to that of the PES in the asymptotic region of the product channel, that is, it is angularly isotropic.

In order to understand how the product of different rotational states were produced, the wave function of the product HF (v_{HF} = 2) was decomposed into three components, by projection the reactive resonance wave function with the ro-vibrational state of (v_{HF}, j_{HF}) = (2, 0−3), (2, 4−7), and (2, 8−13). The corresponding plots are presented in Figure 4C, D, and E. It is observed clearly there that, these three components of the "emitted" wave function from the resonance region have different starting positions, from which they acquire angular momentum of different amplitudes as evidenced by the observation that they move along the angular degree of freedom with different velocities when they go to product asymptotic region. As a result, there is a broad rotational state distribution of the final product HF (v_{HF} = 2), which ultimately exhibits trimodal structure, possibly by quantum interference.

Similar plots of the resonance wave function of the F + H_2 reaction at collision energy of 0.115 kcal/mol with J_{total} = 0 are given in Figure 5A, B, C, and D, but in panel A the PES is obtained with r_{HF} = 2.3 au where the resonance wave function has largest amplitude. Now it is observed that the product is emitted out with much smaller angular kinetic energy because the wave function moves slowly along the angular degree of freedom as it goes to the asymptotic region, in contrast with those shown in Figure 4.

A careful comparison between the plots in Figure 4B and Figure 5B, shows that a considerable part of the wave function around R_{D-HF} = 4.0 au in Figure 4B extends into the region of highly rotational excited states. In contrast, the component of the wave function of highly rotational excited states around R_{H-HF} = 4.0 au in Figure 5B is much smaller. A rough picture of the relative populations in different rotational states of the resonance wave function is given in Figure 6A and B, which presents some 1D plots of the wave function $|\varphi(\theta)|^2$ at fixed $R_{D/H-HF}$ where the wave function has largest amplitude along the $R_{D/H-HF}$ degree of freedom. Figure 6 tells us clearly that for the F + H_2 reaction, the resonance wave function concentrates at j_{HF} = 0−8 states and only has a negligible part with j_{HF} = 9−14. However, there is a considerable part of the wave function with j_{HF} = 8−14 for the resonance state of the F + HD reaction.

The markedly different rotational state distributions between the resonance states of the F + HD and F + H_2 reactions can be traced back to the difference in their local PESs around resonance region. From the panel A of Figures 4 and 5, due to the difference in the length of the H—F bond (2.3 au in the F + H_2 versus 2.5 au in the F + HD), we see that the angular potential well at $R_{D—HF/H—HF}$ = 4.0 au is much deeper in the F + HD reaction, which supports the resonance state with more angular kinetic energy.

Because for the resonance wave functions of both reactions, the part with highly rotational excited states goes into product region efficiently, the rotational states distribution of HF (v_{HF} = 2) for these two reactions ultimately exhibit markedly different structures and the HF from the reaction F + HD is much more rotational excited.

As we understand, a well-isolated reactive resonance state in a chemical reaction can be well regarded being as the photon excited state in a photodissoiation process. This state controls the reactive scattering process, determines the product channel ratios, product scattering direction, and so forth, similar to the photon-exited state. In some particular case, the reactive scattering product may be predicted by the resonance states of a few of partial waves or even single partial wave, similar to a photodissociation process.[33] The difference between them is that a photodissociation can only happen through the excited state, which has considerable Franck−Condon (FC) factor with a definite initial state. However, in a reactive scattering, the resonance state is produced by reactive collisions in crossed molecular beams and, thus, is "excited" by its reactivity instead of photon, and usually involves more than one partial waves.

Due to the connection of a resonance state with the initial state of reagents, we attempt to explain the physical origin for the different features of the resonance wave function of these

dx.doi.org/10.1021/jz501460k | J. Phys. Chem. Lett. 2014, 5, 3049−3055

two reactions using schemes in Figure 7. Before the transition state, the F atom collides with HD/H_2 in a direction

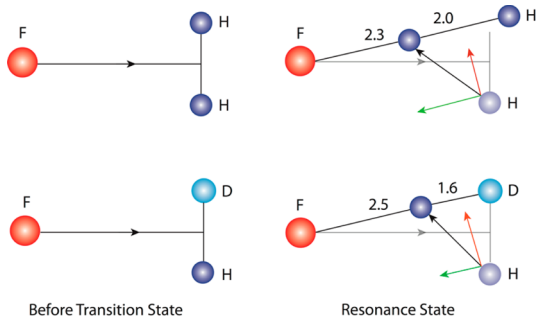

Figure 7. Schemes illustrating the different velocities, which are parallel (green arrows) and perpendicular (red arrows) with the axis of F−H−D/H, acquired by the H atom in the reaction of F + HD/H_2 reaction. Please note the significant difference in the distances between the H−H atoms and H—D atoms of the resonance states.

perpendicular to the bond of the diatomic reagent, restricted by the van der Waals well in the entrance channel and its low translational energy in the case of present study[16,34] (see Figure S4 of the Supporting Information). Because the resonance occurs through the tunneling effect (the static barrier height is about 1.72 kcal/mol on the CSZ PES, which is much higher than the applied collision energies), the H atom jumps through the transition barrier rapidly from the van der Waals well to form the resonance state in a collinear configuration. In contrast with the F + H_2 reaction, the H atom in the F + HD reaction moves to a position a little farther away from the F atom. At the same time, the distance between the H and D atom in the F + HD reaction is much shorter than that between the H and H atom in the F + H_2 reaction because the D atom hardly moves its position during the H tunneling process. The tunneled H atom in the F + HD reaction acquires much more velocity perpendicular with the axis of F−H−D than that in the F + H_2 reaction because total available energy for producing HF is comparable for these two reactions. On the contrary, the H atoms in the F + H_2 reaction acquires much more velocity parallel with the axis of F−H−H. As a result, the product HF of the F + HD reaction is more rotational excited but the F + H_2 reaction tends to produce HF with higher vibrational excited states.

■ ASSOCIATED CONTENT

Supporting Information

Graphs for TOF spectra, integral cross sections of product HF ($v' = 2$) of the two titled reactions, rotational state distributions of HF ($v' = 2$) in the energy range mediated by the resonance states, and reactive resonance wave functions in the reactant channel. This material is available free of charge via the Internet at http://pubs.acs.org.

■ AUTHOR INFORMATION

Corresponding Authors

*E-mail: chunleixiao@dicp.ac.cn.
*E-mail: zsun@dicp.ac.cn.
*E-mail: xmyang@dicp.ac.cn.
*E-mail: zhangdh@dicp.ac.cn.

Notes

The authors declare no competing financial interest.

■ ACKNOWLEDGMENTS

This work was supported by the National Natural Science Foundation of China, the Ministry of Science and Technology of China, and the Chinese Academy of Sciences.

■ REFERENCES

(1) Schatz, G. C.; Bowman, J. M.; Kupperma, A. Large Quantum Effects in Collinear F + H_2 → FH + H Reaction. *J. Chem. Phys.* **1973**, *58*, 4023−4025.
(2) Schatz, G. C.; Bowman, J. M.; Kuppermann, A. Exact Quantum, Quasiclassical, and Semiclassical Reaction Probabilities for Collinear F + H_2 → FH + H Reaction. *J. Chem. Phys.* **1975**, *63*, 674−684.
(3) Wu, S. F.; Johnson, B. R.; Levine, R. D. Quantum-Mechanical Computational Studies of Chemical Reactions 0.3. Collinear A + BC Reaction with Some Model Potential-Energy Surfaces. *Mol. Phys.* **1973**, *25*, 839−856.
(4) Neumark, D. M.; Wodtke, A. M.; Robinson, G. N.; Hayden, C. C.; Lee, Y. T. Experimental Investigation of Resonances in Reactive Scattering—the F + H_2 Reaction. *Phys. Rev. Lett.* **1984**, *53*, 226−229.
(5) Neumark, D. M.; Wodtke, A. M.; Robinson, G. N.; Hayden, C. C.; Lee, Y. T. Molecular-Beam Studies of the F + H_2 Reaction. *J. Chem. Phys.* **1985**, *82*, 3045−3066.
(6) Manolopoulos, D. E.; Stark, K.; Werner, H. J.; Arnold, D. W.; Bradforth, S. E.; Neumark, D. M. The Transition-State of the F + H_2 Reaction. *Science* **1993**, *262*, 1852−1855.
(7) Chapman, W. B.; Blackmon, B. W.; Nesbitt, D. J. State-to-State Reactive Scattering of F + H_2 in Supersonic Jets: Nascent Rovibrational HF(v, J) Distributions via Direct IR Laser Absorption. *J. Chem. Phys.* **1997**, *107*, 8193−8196.
(8) Liu, K. Quantum Dynamical Resonances in Chemical Reactions: From A + BC to Polyatomic Systems. In *Advances in Chemical Physics*; John Wiley & Sons, Inc.: New York, 2012; pp 1−46.
(9) Lynch, G. C.; Steckler, R.; Schwenke, D. W.; Varandas, A. J. C.; Truhlar, D. G.; Garrett, B. C. Use of Scaled External Correlation, a Double Many-Body Expansion, and Variational Transition-State Theory to Calibrate a Potential-Energy Surface for FH_2. *J. Chem. Phys.* **1991**, *94*, 7136−7149.
(10) Aoiz, F. J.; Banares, L.; Herrero, V. J.; Rabanos, V. S.; Stark, K.; Werner, H. J. Classical Dynamics for the F + H_2 →HF + H Reaction on a New Ab-Initio Potential-Energy Surface— A Direct Comparison with Experiment. *Chem. Phys. Lett.* **1994**, *223*, 215−226.
(11) Stark, K.; Werner, H. J. An Accurate Multireference Configuration Interaction Calculation of the Potential Energy Surface for the F + H_2 → HF + H Reaction. *J. Chem. Phys.* **1996**, *104*, 6515−6530.
(12) Castillo, J. F.; Manolopoulos, D. E.; Stark, K.; Werner, H. J. Quantum Mechanical Angular Distributions for the F + H_2 Reaction. *J. Chem. Phys.* **1996**, *104*, 6531−6546.
(13) Xu, C. X.; Xie, D. Q.; Zhang, D. H. A Global Ab Initio Potential Energy Surface for F + H_2 → HF + H. *Chin. J. Chem. Phys.* **2006**, *19*, 96−98.
(14) Polanyi, J. C. Some Concepts in Reaction Dynamics. *Acc. Chem. Res.* **1972**, *5*, 161−168.
(15) Skodje, R. T.; Skouteris, D.; Manolopoulos, D. E.; Lee, S. H.; Dong, F.; Liu, K. P. Resonance-Mediated Chemical Reaction: F + HD → HF + D. *Phys. Rev. Lett.* **2000**, *85*, 1206−1209.
(16) Skodje, R. T.; Skouteris, D.; Manolopoulos, D. E.; Lee, S. H.; Dong, F.; Liu, K. Observation of a Transition State Resonance in the Integral Cross Section of the F + HD Reaction. *J. Chem. Phys.* **2000**, *112*, 4536−4552.
(17) Qiu, M. H.; Ren, Z. F.; Che, L.; Dai, D. X.; Harich, S. A.; Wang, X. Y.; Yang, X. M.; Xu, C. X.; Xie, D. Q.; Gustafsson, M.; et al. Observation of Feshbach Resonances in the F + H_2 → HF + H Reaction. *Science* **2006**, *311*, 1440−1443.
(18) Lee, S. H.; Dong, F.; Liu, K. P. Reaction Dynamics of F + HD → HF + D at Low Energies: Resonant Tunneling Mechanism. *J. Chem. Phys.* **2002**, *116*, 7839−7848.

(19) Lee, S.-H.; Dong, F.; Liu, K. A Crossed-Beam Study of the F + HD → HF + D Reaction: The Resonance-Mediated Channel. *J. Chem. Phys.* **2006**, *125*, 133106−10.
(20) Wang, X.; Dong, W.; Qiu, M.; Ren, Z.; Che, L.; Dai, D.; Wang, X.; Yang, X.; Sun, Z.; Fu, B.; et al. HF(v'=3) Forward Scattering in the F + H_2 Reaction: Shape Resonance and Slow-down Mechanism. *Proc. Natl. Acad. Sci. U. S. A.* **2008**, *105*, 6227−6231.
(21) Ren, Z.; Che, L.; Qiu, M.; Wang, X.; Dong, W.; Dai, D.; Wang, X.; Yang, X.; Sun, Z.; Fu, B.; et al. Probing the Resonance Potential in the F Atom Reaction with Hydrogen Deuteride with Spectroscopic Accuracy. *Proc. Natl. Acad. Sci. U. S. A.* **2008**, *105*, 12662−12666.
(22) Fu, B.; Xu, X.; Zhang, D. H. A Hierarchical Construction Scheme for Accurate Potential Energy Surface Generation: An Application to the F + H_2 Reaction. *J. Chem. Phys.* **2008**, *129*, 011103−4.
(23) Chen, J.; Sun, Z.; Zhang, D. Accurate Global Potential Energy Surface for F + H_2 Reaction. *J. Chem. Phys.*; to be submitted for publication.
(24) Wang, T.; Chen, J.; Yang, T. G.; Xiao, C. L.; Sun, Z. G.; Huang, L.; Dai, D. X.; Yang, X. M.; Zhang, D. H. Dynamical Resonances Accessible Only by Reagent Vibrational Excitation in the F Plus HD → HF Plus D Reaction. *Science* **2013**, *342*, 1499−1502.
(25) Schnieder, L.; SeekampRahn, K.; Wrede, E.; Welge, K. H. Experimental Determination of Quantum State Resolved Differential Cross Sections for the Hydrogen Exchange Reaction H + D_2 → HD + D. *J. Chem. Phys.* **1997**, *107*, 6175−6195.
(26) Qiu, M. H.; Che, L.; Ren, Z. F.; Dai, D. X.; Wang, X. Y.; Yang, X. M. High Resolution Time-of-Flight Spectrometer for Crossed Molecular Beam Study of Elementary Chemical Reactions. *Rev. Sci. Instrum.* **2005**, *76*, 083107−5.
(27) Ren, Z. F.; Qiu, M. H.; Che, L.; Dai, D. X.; Wang, X. Y.; Yang, X. M. A Double-Stage Pulsed Discharge Fluorine Atom Beam Source. *Rev. Sci. Instrum.* **2006**, *77*, 016103−3.
(28) Valiev, M.; Bylaska, E. J.; Govind, N.; Kowalski, K.; Straatsma, T. P.; Van Dam, H. J. J.; Wang, D.; Nieplocha, J.; Apra, E.; Windus, T. L.; et al. NWChem: A Comprehensive and Scalable Open-Source Solution for Large Scale Molecular Simulations. *Comput. Phys. Commun.* **2010**, *181*, 1477−1489.
(29) Yang, X. M.; Zhang, D. H. Probing Quantum Dynamics of Elementary Chemical Reactions via Accurate Potential Energy Surfaces. *Z. Phys. Chem.* **2013**, *227*, 1247−1265.
(30) Sun, Z.; Guo, H.; Zhang, D. H. Extraction of State-to-State Reactive Scattering Attributes from Wave Packet in Reactant Jacobi Coordinates. *J. Chem. Phys.* **2010**, *132*, 084112−11.
(31) Skouteris, D.; Castillo, J. F.; Manolopoulos, D. E. ABC: A Quantum Reactive Scattering Program. *Comput. Phys. Commun.* **2000**, *133*, 128−135.
(32) Skodje, R. T.; Sadeghi, R.; Köppel, H.; Krause, J. L. Spectral Quantization of Transition State Dynamics for the Three-Dimensional H + H_2 Reaction. *J. Chem. Phys.* **1994**, *101*, 1725−1729.
(33) Dong, W.; Xiao, C.; Wang, T.; Dai, D.; Yang, X.; Zhang, D. H. Transition-State Spectroscopy of Partial Wave Resonances in the F Plus HD Reaction. *Science* **2010**, *327*, 1501−1502.
(34) Aoiz, F. J.; Bañares, L.; Herrero, V. J.; Sáez Rábanos, V.; Stark, K.; Werner, H. J. The F + HD → DF(HF) + H(D) Reaction Revisited: Quasiclassical Trajectory Study on an Ab Initio Potential Energy Surface and Comparison with Molecular Beam Experiments. *J. Chem. Phys.* **1995**, *102*, 9248−9262.